Research paper

Title: Development of a non-viral platform for rapid virus-like particle production in Sf9 cells

Author names and affiliations: Puente-Massaguer, Eduard[1]; Gòdia, Francesc[1]; Lecina, Martí[2]

[1]Departament d'Enginyeria Química, Biològica i Ambiental, Universitat Autònoma de Barcelona, Cerdanyola del Vallès, Barcelona, Spain

[2]IQS School of Engineering, Universitat Ramón Llull, Barcelona, Spain

Corresponding author: Eduard Puente-Massaguer

E-mail: eduard.puente.massaguer@gmail.com

ORCID: 0000-0002-2816-7051

Address: Departament d'Enginyeria Química, Biològica i Ambiental, Escola d'Enginyeria, Universitat Autònoma de Barcelona, Cerdanyola del Vallès, Barcelona, Spain

Abstract

Insect cells have shown a high versatility to produce multiple recombinant products. The ease of culture, low contamination risk with human pathogens and high expression capacity makes an attractive platform to generate virus-like particles (VLPs). The baculovirus expression vector system (BEVS) has been frequently used to produce these complex nanoparticles. However, the BEVS entails several difficulties in the downstream phase as well as undesirable side-effects due to the expression of baculovirus-derived proteins. In this work, we developed a baculovirus-free system based on polyethylenimine (PEI)-mediated transient gene expression (TGE) of Sf9 cells. An exhaustive study of DNA:PEI polyplex formation was performed and the optimal TGE conditions were determined by the combination of Design of Experiments (DoE) and desirability functions. The TGE approach was successfully applied to produce three model recombinant products with different structural complexities, including eGFP, hSEAP and HIV-1 Gag VLPs. Cell membrane co-localization with the Gag polyprotein was detected by fluorescence microscopy, whereas nanoparticle tracking analysis and flow virometry were applied as high-throughput techniques to monitor the VLP production process. Analysis of VLP production revealed that 48 h after transfection were optimal for VLP harvesting since the ratio of VLPs to extracellular vesicles was the highest. In these conditions, a maximum of 1.9 ± $0.8 \cdot 10^9$ VLP/mL was achieved, representing a 2.8-fold increase compared to the initial transfection condition. In conclusion, the TGE approach proposed in this study provides a baculovirus-free platform to rapidly produce VLPs and potentially other recombinant products in insect cells.

Keywords: Virus-like particle, Sf9 cells, Transient gene expression, Cryo-transmission electron microscopy, Flow virometry, Polyethylenimine.

Abbreviations: ANOVA, analysis of variance; BEVS, baculovirus expression vector system; Cryo-TEM, cryo-transmission electron microscopy; DoE, Design of Experiments; eGFP, enhanced green fluorescent protein; HIV, human immunodeficiency virus; hpt, hours post transfection; hSEAP, human secreted alkaline phosphatase; LOF, lack-of-fit; NTA, nanoparticle tracking analysis; PEI, polyethylenimine; SN, supernatant; TGE, transient gene expression; VLP, virus-like particle.

1. Introduction

The development of rapid and efficient systems for recombinant protein production is essential to meet the increasing demand in biotechnological products. Animal cell lines are frequently used to this purpose since many of the recombinant proteins require complex post-translational modifications (Gutierrez and Lewis, 2015). The insect cell/baculovirus expression vector system (BEVS) is extensively used considering that high production yields can be achieved in short time-frames. Moreover, insect cells are easy to culture, can tolerate higher levels of osmolarity and by-product concentrations, and provide a greater level of biosafety compared to mammalian cells due to the absence of known human pathogens (Ikonomou et al., 2003). Common insect cell lines used with the BEVS belong to the order of the Lepidoptera, mainly Sf9 cells from *Spodoptera frugiperda* and High Five cells from *Trichoplusia ni*. Several recombinant products have been produced using this strategy, from simple (George et al., 2015) to more complex ones such as G-protein-coupled receptors (Carpentier et al., 2001) and virus-like particles (VLPs) (Nika et al., 2017). However, the baculovirus infection cycle jeopardizes cell integrity, product quality due to protease release, and the separation of complex nanoparticles from the baculovirus itself is hindered (Lin et al., 2014). In addition, the BEVS is time-consuming for high-throughput screening applications mainly due to the effort in developing and titrating the baculovirus working stock (Bleckmann et al., 2016a).

In this context, the use of new production methodologies free of baculoviruses is of general interest. Transient gene expression (TGE) has proved to achieve moderate to high concentrations of several recombinant products in mammalian cell lines (Gutiérrez-Granados et al., 2018). Nevertheless, less information is available regarding their performance in insect cell lines. Initial transfection experiments of insect cells were performed in adherent cultures using liposome-based reagents in most cases (Keith et al., 1999; Lu et al., 1996). Despite the initial efforts with these transfection carriers at small scale, difficulties are encountered in process scale-up due to their high cost. Polyethylenimine (PEI) has demonstrated to work adequately as transfection reagent for a handful of animal cell lines (Geisse, 2009). Recently, the successful

production of several simple recombinant proteins by PEI-mediated TGE in suspension-adapted insect cells has been reported (Bleckmann et al., 2019; Mori et al., 2017; Shen et al., 2015, 2013). However, the benefit of using this system as a platform to produce complex nanoparticles such as VLPs has not yet been investigated.

In the current study, we have developed a PEI-mediated TGE approach for Sf9 cells using a low-hydrolysate culture medium in order to reduce experimental variability and ensure the reliability of the process. The plasmid vector used for TGE is pIZTV5, which harbors the immediate-early *Op*IE2 promoter, with positive results recently reported for transient protein production in High Five cells (Bleckmann et al., 2019; Puente-Massaguer et al., 2018). The first part of the study is focused on the investigation of the DNA:PEI polyplex formation conditions mediating Sf9 cell transfection by cryogenic transmission electron microscopy (cryo-TEM) and spectrofluorometry. Then, a rational approach is used to detect the synergies between the main variables influencing the production process and determine an optimal condition for TGE. To this end, a combination of Design of Experiments (DoE) and multiple response analysis using desirability functions is applied. The reproducibility of the TGE condition is successfully validated with three different recombinant products: intracellular enhanced green fluorescent protein (eGFP), human secreted alkaline phosphatase (hSEAP) and the human immunodeficiency virus (HIV-1) Gag polyprotein responsible for VLP formation. The *gag* gene is fused in frame to eGFP with the aim to facilitate the detection of Gag-eGFP in the cell membrane and release in the form of assembled VLPs. This process is thoroughly monitored and characterized by multiple analytical tools, including confocal microscopy, nanoparticle tracking analysis (NTA) and flow virometry. The methodology here proposed represents an advance for VLP production in insect cells devoid of the BEVS, and should facilitate the downstream processing of these complex nanoparticles as well as other recombinant products.

2. Materials and methods

2.1 Cell culture conditions

The suspension-adapted Sf9 cell line (cat. num. 71104, Merck, Darmstadt, Germany) used in this work was kindly provided by Dr. Nick Berrow (Institute for Research in Biomedicine, Barcelona, Spain). Cells were adapted to the low-hydrolysate Sf900III medium (Thermo Fisher Scientific, Grand Island, NY, USA) and subcultured three times a week at a density of 4 – 6 x 10^5 cells/mL in 125/250-mL disposable polycarbonate Erlenmeyer flasks (Corning, Steuben, NY, USA). All cultures were shaken at 130 rpm using an orbital shaker (Stuart, Stone, UK) and maintained at 27°C as previously described (Puente-Massaguer et al., 2020a). Cell count and viability were measured daily with the Nucleocounter NC-3000 (Chemometec, Allerød, Denmark).

2.2 Plasmid vectors

The plasmid vector used in this work was pIZTV5 (cat. num. V801001, Thermo Fisher Scientific) which contains the immediate-early *Op*IE2 promoter. The genes encoding for the intracellular enhanced green fluorescent protein (eGFP), the truncated form of the human secreted alkaline phosphatase (hSEAP) and the human immunodeficiency virus (HIV-1) Gag fused in frame to the eGFP were cloned into this vector using standard cloning procedures. Briefly, the *hSEAP* gene was PCR amplified from pUNO1-hSEAP plasmid (InvivoGen, San Diego, CA, USA) using the following primer pair: fwd 5'-CGTAGGTACCTCATGATTCTGGGGCCCTGC-3', rev 5'-CGTAGCGGCCGCGTCCAAACTCATCAATGTATC-3'. The amplified fragment was digested with *Kpn*I and *Not*I and ligated resulting in the pIZTV5-hSEAP plasmid. The *gag-eGFP* gene was obtained by digesting the pGag-eGFP plasmid (cat. num. 11468, NIH AIDS Reagent Program) with *Kpn*I and *Not*I obtaining the pIZTV5-Gag-eGFP plasmid after ligation. The pIZTV5-eGFP plasmid was developed as previously reported (Puente-Massaguer et al., 2018).

149

150 *2.3 Transient gene expression*

151 Sf9 cells were transiently transfected with the different plasmid DNA using 25 kDa linear
152 polyethylenimine (PEI, PolySciences, Warrington, PA, USA). The 25 kDa linear PEI stock
153 solution was prepared in ultrapure water at a concentration of 1 mg/mL with a final pH of 7 and
154 sterilized by filtration. The initial transfection protocol was defined according to initial
155 transfection experiments (Fig. S1 – S2). Exponentially growing cells at 4 x 10^6 cell/mL were
156 centrifuged at 300 x*g* for 5 min and concentrated by a factor of 5 (20 x 10^6 cell/mL) in 8 mL of
157 pre-warmed Sf900III medium. DNA and PEI polyplex formation was performed in 0.8 mL of
158 incubation solution with DNA added first at 1 pg/cell and vortexed for 10 s. Then PEI was
159 added to DNA at 2 pg/cell and vortexed 3 s 3 times. After 10 min of incubation at room
160 temperature, the mixture was added to the concentrated culture for 1 h and then diluted to 4 x
161 10^6 cell/mL with Sf900III medium. Different incubation solutions were tested for DNA:PEI
162 polyplex formation, including 150 mM NaCl (Sigma Aldrich, Saint Louis, MO, USA), ultrapure
163 water (Merck Millipore, Burlington, MA, USA) and Sf900III medium.

164

165 *2.4 Flow cytometry*

166 The percentage of eGFP and Gag-eGFP expressing cells was assessed using a BD FACS Canto
167 II flow cytometer equipped with a 488 nm laser configuration (BD Biosciences, San Jose, CA,
168 USA). The number of eGFP and Gag-eGFP positive cells was determined in the FITC PMT
169 detector (Puente-Massaguer et al., 2020b).

170

171 *2.5 Fluorescence confocal microscopy*

172 eGFP and Gag-eGFP transfected cells were observed using a TCS SP5 confocal microscope
173 (Leica, Wetzlar, Germany). To do this, cells were stained with 0.1 % v/v of CellMask™ and 0.1
174 % v/v of Hoechst 33342 (Thermo Fisher Scientific) for lipid membrane and cell nucleus
175 visualization, respectively. A washing step was performed to remove dye excess by centrifuging

the cells at 300 x*g* for 5 min and resuspending them in fresh Sf900III medium. Samples were placed in 35 mm glass bottom Petri dishes with 14 mm microwell (MatTek Corporation, Ashland, MA, USA) for visualization.

2.6 Fluorescence quantification by spectrofluorometry

The supernatant of eGFP and Gag-eGFP producing cells was harvested by centrifugation at 3000 x*g* for 5 min. Pelleted cells were then subjected to three freeze-thaw cycles for intracellular eGFP and Gag-eGFP measurement. Green fluorescence was measured with a Cary Eclipse fluorescence spectrophotometer (Agilent Technologies, Santa Clara, CA, USA) at room temperature set as follows: λ_{ex} = 488 nm (5 nm slit), λ_{em} = 500 – 530 nm (10 nm slit). Relative fluorescence unit values (R.F.U.) were calculated by subtracting fluorescence unit values of negative non-transfected cultures. eGFP concentration was determined using a standard curve based on a linear correlation of known eGFP concentrations (BioVision, Milpitas, CA, USA) and the associated fluorescence intensity in R.F.U. (Fig. S4):

eGFP (mg/L) = (R.F.U. – 6.7221)/59.144 (1)

where eGFP is the estimated concentration of eGFP protein and R.F.U. is the measured eGFP fluorescence intensity in the samples.

A correlation was also established between R.F.U. from Gag-eGFP transfected Sf9 cell supernatants and VLPs (fluorescent particles) measured by NTA:

Gag-eGFP VLPs (fluorescent particles/mL) = 3.96 x 10^8 · R.F.U. (2)

The Sf900III medium and a 0.1 mg/mL quinine sulphate solution were used as control patterns to normalize R.F.U. values between different experiments.

2.7 hSEAP quantification

The supernatant of hSEAP producing cells was harvested by centrifugation at 3000 x*g* for 5 min and cell pellets were disrupted for intracellular hSEAP measurement as described in the previous section. The alkaline phosphatase activity was assessed with a colorimetric enzyme

reaction using the QUANTI-Blue system (InvivoGen). To do this, 20 µL of sample were added to 200 µL of pre-warmed QUANTI-Blue solution and incubated for 1 h at 37 ºC. The absorbance was measured in a Victor^3 spectrophotometer (PerkinElmer, Waltham, MA, USA) at a wavelength of 620 nm. Relative activity units (R.A.U.) were calculated by subtracting the absorbance of non-transfected cultures. The hSEAP concentration was determined by using a calibration curve based on a linear correlation of known hSEAP concentrations (InvivoGen) and the corresponding activity units in R.A.U.:

$$hSEAP\ (mg/L) = R.A.U. \times 2.9744 + 0.0615 \quad (3)$$

where hSEAP is the estimated concentration of hSEAP protein and R.A.U. is the measured hSEAP activity units in the samples.

2.8 Enzyme-linked immunosorbent assay (ELISA)

HIV-1 p24 concentrations from Gag-eGFP transfected Sf9 cell supernatants and pellets were determined by HIV-1 p24 ELISA (Sino Biological, Wayne, NJ, USA). Supernatants were harvested by centrifugation at 3000 x*g* for 5 min and cell pellets were disrupted as previously described. Samples were incubated with SNCR buffer (Schüpbach et al., 2006) for 10 min at 70 °C and incubated with 1.5 % Triton X-100 for 10 min at 100 °C to disrupt the nanoparticles. The substrate solution was prepared by dissolving a SIGMA*FAST* OPD substrate tablet (Sigma Aldrich) and one urea hydrogen peroxide tablet (Sigma Aldrich) in deionized water at a final concentration of 0.4 mg/mL. An HIV-1 p24 standard of known concentration was also included to calculate the Gag-eGFP concentration (cat. num. ab9071, Abcam, Cambridge, United Kingdom). The reaction was stopped adding a 625 mM H_2SO_4 solution (Merck). The absorbance was measured at 492 nm with a reference wavelength of 630 nm in a Tecan Infinite 200 Pro reader (Tecan, Männedorf, Switzerland) as described by Reiter and co-workers (Reiter et al., 2019). p24 concentration values were corrected according to the Gag-eGFP molecular weight (87.7 kDa).

2.9 Cryo-transmission electron microscopy

Morphology and qualitative particle size of DNA:PEI polyplexes were visualized with a transmission electron microscope equipped with a cryotransfer holder. Briefly, 4 µL of sample were blotted onto EMR Holey carbon films on 400 mesh copper grids (Micro to Nano, Wateringweg, the Netherlands) for 3 s and 77 % relative air humidity. Grids were previously subjected to a glow discharge treatment in a PELCO easiGlow™ Discharge Cleaning System (PELCO, Fresno, CA, USA). Samples were subsequently plunged into liquid ethane at −180 °C using a Leica EM GP workstation (Leica, Wetzlar, Germany) and observed in a JEM-2011 TEM operating at 200 kV (Jeol Ltd., Akishima, Tokyo, Japan). Samples were maintained at −180 °C during imaging and pictures were taken using a CCD 895 USC 4000 multiscan camera (Gatan, Pleasanton, CA, USA).

2.10 Particle quantification by nanoparticle tracking analysis

The number of VLPs (fluorescent particles) and total nanoparticles present in Gag-eGFP harvested supernatants at 48 hpt was measured using a NanoSight NS300 (Malvern Panalytical, Malvern, United Kingdom). Samples were diluted in 0.22 µm-filtered DPBS (Thermo Fisher Scientific) and continuously injected into the device chamber through a pump at an average concentration of 10^8 particles/mL (20 – 60 particles/frame). Videos of 60 s from independent triplicate measurements were analyzed with the NanoSight NTA 3.2 software.

2.11 Particle quantification using flow virometry

The production process of VLPs and other nanoparticles from Gag-eGFP harvested supernatants was measured using a CytoFlex LX flow cytometer (Beckman Coulter, Brea, CA, USA) equipped with a 488 nm blue laser for fluorescent particle detection and a 405 nm laser/violet side scatter configuration for improved nanoparticle size resolution. Samples were diluted in

0.22 µm-filtered DPBS and triplicate measurements from independent samples were analyzed with the CytExpert 2.3 software.

2.12 VLP characterization through sucrose cushion ultracentrifugation

The supernatant of Gag-eGFP transfected Sf9 cells at 48 hpt was sublayered with 5 mL of 25 % and 8 mL of 45 % (w/v) sucrose (Sigma Aldrich) solution prepared in DPBS or DMEM (Thermo Fisher Scientific), respectively. 10 mL of supernatant were loaded in an ultracentrifuge tube (Beckman Coulter), filled to the top with sterile DPBS and centrifuged at 31000 rpm for 2.5 h at 4 ºC (Optima L100XP, SW 32 Ti rotor, Beckman Coulter). Samples were taken from each one of the ultracentrifugation fractions and pellets were resuspended in 100 µL of sterile DPBS overnight. All samples were stored either at -4 or -80 ºC.

2.13 DoE-based optimization of TGE

A three-variable Box-Behnken design was selected to find the optimal conditions for eGFP production (R.F.U.), transfection (% of eGFP positive cells) and cell viability (% of viable cells after transfection). Viable cell concentration at transfection (10^6 cell/mL), DNA/cell and PEI/cell ratio (pg/cell) were chosen as the critical variables of the study (Liu et al., 2008). These variables were screened at three levels coded as: low level (-1), medium level (0) and high level (+1) (Table 1). Data were fitted to a second-order polynomial equation for each response by linear regression analysis (Eq. 4):

$$Y = \beta_0 + \sum_{i=1}^{k} \beta_i \cdot X_i + \sum_{i=1}^{k} \beta_{ii} \cdot X_i^2 + \sum_{i=1}^{k} \sum_{j>1}^{k} \beta_{ij} \cdot X_i \cdot X_j + \varepsilon \quad (4)$$

where Y corresponds to each response under consideration (eGFP production, transfection and cell viability), β_0 is the model intercept term, β_i the linear coefficient, β_{ii} the quadratic coefficient, β_{ij} the interaction coefficient, X_i and X_j the studied variables (viable cell concentration at transfection, DNA/cell and PEI/cell ratio) and ε the experimental error. Data

fitting for each response was performed in R language environment (R Foundation for Statistical Computing, Vienna, Austria).

The best condition for TGE was found by simultaneously considering the three response functions obtained based on equation 4 with a modified version of the *desirability* package in R. Different ranges were selected for each response according to experimental data and a weight value (*s*-value) was also chosen depending on the relevance given to the fitted equation (Eq. 5):

$$d_n = \begin{cases} 0 & if\ Y_n < LL \\ \left(\frac{Y_n - LL}{UL - LL}\right)^s & if\ LL \leq Y_n \leq UL \\ 1 & if\ Y_n > UL \end{cases} \quad (5)$$

where d_n is the desirability function for each equation, *s* refers to the relevance value given to the equation, Y_n is the fitted equation and *LL* and *UL* are the lower and upper limits of each equation, respectively. The different *n* desirability functions were then combined to find the conditions that maximize the Overall Desirability (*OD*) function (Puente-Massaguer et al., 2018).

2.14 Statistical analyses

Statistical analyses of the different equations were performed using R software. The quality of the regression of the fitted equations was evaluated with the R^2 and R^2_{adj} coefficients. An analysis of variance (ANOVA) *F*-test was used to determine the significance of the equations and each of the coefficients involved was assessed with a *t*-test. The lack-of-fit (LOF) test was used to evaluate differences between the experimental and pure error of the fitted equations. A *p*-value < 0.05 was considered statistically significant with a 95 % confidence.

3. Results

3.1 Preliminary screening of transfection conditions

Several toxicity assays were conducted to define the appropriate DNA and PEI concentration ranges for Sf9 cells in Sf900III medium (Fig. S1). Initial series of transfection studies were

performed at exponential phase (3 x 10^6 cell/mL) using the pIZTV5-eGFP plasmid but low transfections were achieved (< 20 %). At the same time, cell viability was compromised with increasing PEI concentrations. Medium replacement before transfection enabled the obtaining of higher transfection efficiencies (20 – 30 %) as well as cell viabilities after transfection. Remarkably, a substantial improvement in transfection efficacy was attained at high cell concentrations (30 – 40 %) being the strategy adopted in the following optimization studies (Fig. S2).

3.2 Study of DNA:PEI complexing on transient gene expression (TGE)

It is widely accepted that the efficiency of DNA:PEI polyplexes on transfection is influenced by the solution used for complexation (Van Gaal et al., 2011). To this purpose, different solutions including ultrapure water, Sf900III medium and 150 mM NaCl were tested. Sequential addition of PEI and DNA to the cell culture (no complexing) was also investigated since it has been reported to work in different cell lines (Hacker et al., 2013). Best transfection efficiencies were achieved at 48 – 72 hours post transfection (hpt) with DNA and PEI incubation in ultrapure water and without DNA:PEI complexing (Fig. 1b). In both conditions, a decrease in cell growth rate was observed. Interestingly, cells transfected with pre-formed DNA:PEI polyplexes were more fluorescent in all cases compared to the no complexing condition (Fig. 1c). This was translated into a higher level of eGFP production in polyplexes pre-formed in ultrapure water though similar transfection efficiencies were attained without DNA:PEI complexing (Fig. 1d). Maximum intracellular eGFP production was accomplished at 72 hpt and barely no eGFP was detected in the supernatant (Fig. 1d, S3a). According to these results, ultrapure water was selected as the incubation solution for DNA:PEI polyplex formation since the best transfection efficiency and eGFP production were achieved.

The DNA:PEI polyplex incubation time was assessed to determine the best conditions for an optimal transfection. To evaluate this, a transfection experiment with polyplexes incubated for <1, 10, 20 and 30 min in ultrapure water was performed. No differences were observed among

the different conditions tested (Fig. S3b – c). In this sense, the strategy adopted for polyplex formation consisted in mixing DNA with PEI and immediately adding them to the concentrated culture. Cryo-TEM was used to characterize the morphology and size of these polyplexes in native conditions, which could be observed as black electron-dense structures with an heterogeneous size comprised in the 0.2 – 1.5 µm range (Fig. 2a – b).

Transfection at high cell concentrations required the use of high PEI concentrations to maintain the PEI/cell ratio. To decrease the risk of cell damage upon prolonged exposure to these conditions, Sf9 concentrated cell cultures were transfected with polyplexes and incubated for 15, 30, 45 and 60 min before dilution to 4 x 10^6 cell/mL, with the aim to determine the shortest window of time that guaranteed the best transfection conditions. No differences were observed in the transfection yield, but cell viability declined as the incubation time increased from 15 to 45 min (Fig. 2c – d). These results suggested that 15 min of DNA:PEI polyplex incubation with high concentrated cells was adequate to ensure the best level of transfection.

3.3 Optimizing the TGE process

After defining several variables affecting TGE, a DoE approach was implemented to define the optimal conditions maximizing three different objective functions: transfection efficiency (%), cell viability after transfection (%) and eGFP production (R.F.U.). Viable cell concentration at transfection, DNA/cell and PEI/cell ratio were selected as the critical variables influencing the TGE process (Thompson et al., 2012). The different experimental runs of the optimization process were performed with eGFP to facilitate product quantification.

A three-factor Box-Behnken design was generated with ranges for viable cell concentration, DNA/cell and PEI/cell ratio set as 10 – 30 x 10^6 cell/mL, 0.5 – 1.5 pg DNA /cell and 1.5 – 2.5 pg PEI/cell, respectively. The design matrix consisted in 15 experiments in which the central point was triplicated to account for pure experimental error (Table 1). Three different equations based on Eq. 4 were obtained by the least squares' regression method for each one of the

responses under study. Also, the statistical significance of each model equation was confirmed by ANOVA analysis (Table 1).

The best production conditions at 72 hpt were obtained at the highest DNA/cell and PEI/cell ratios (Fig. 3a – c). Indeed, a positive interaction between these two variables was observed. Noticeably, the equation model identified the 10 – 20 x 10^6 cell/mL cell concentration range as the most productive and the optimal production condition was found as 12.9 x 10^6 cell/mL at transfection, 1.3 pg DNA/cell and 2.5 pg PEI/cell ratio. The best transfection efficiency at 72 hpt was obtained at the highest PEI/cell ratio and a viable cell concentration around the medium level (Fig. 3d – f). Interestingly, viable cell concentrations at transfection higher than 20 x 10^6 cell/mL exhibited worse transfection efficiencies even though maintaining the same DNA/PEI and DNA/cell ratios. The optimal condition maximizing Sf9 cell transfection was calculated as 20.4 x 10^6 cell/mL, 0.8 pg DNA/cell and 2.5 pg PEI/cell ratio. Regarding the cell viability at 24 hpt, it was shown to be critical for transfections at high cell concentrations as demonstrated in previous sections. In this case, the variables most significantly influencing viability were viable cell concentration at transfection and PEI/cell ratio. Indeed, high PEI/cell ratios and viable cell concentrations proved to be detrimental for Sf9 cells (Fig. 3g – i). According to these results, the optimal conditions were determined as 10.0 x 10^6 cell/mL, 0.8 pg DNA/cell and 1.5 pg PEI/cell ratio.

The evaluation of TGE in Sf9 cells yielded different optimal conditions depending on the response under consideration. Therefore, a weighted-based equation approach was used to determine a global optimal condition integrating the different responses. Weight assignation to each one of the equations was performed according to a priority criterion (s-value). Preference was equally assigned to production and transfection (s = 2) while a lower restriction was given to cell viability after transfection (s = 1). Responses were then transformed to a d_n scale and combined into a unique overall desirability (OD) function to find a global TGE condition (Eq. 5). This process resulted in 17.6 x 10^6 cell/mL at transfection, 1.0 pg of DNA/cell and 2.0 pg of

PEI/cell ratio with an *OD* score of 0.48. A sensitivity analysis was performed to confirm the robustness of the calculation (data not shown).

3.4 Sf9 cells as a platform to produce VLPs and other recombinant proteins

A confirmation experiment was conducted to verify the global optimal condition (Fig. 4). A maximum eGFP production of 11.7 ± 0.5 mg/L (723.4 ± 40.5 R.F.U.) and a transfection yield of 51.7 ± 4.3 % was obtained at 72 hpt, in agreement with the calculated prediction interval of the DoE (Table 2). Cell culture viability was 79.1 ± 6.7 % at 24 hpt, also in line with the DoE prediction (Fig. 4a). To assess the general applicability of the optimized TGE system here presented, other recombinant products with different structural complexities were assessed. Besides the intracellular eGFP used for process optimization, the production of secreted hSEAP and HIV-1 Gag-eGFP virus-like particles (VLPs) was evaluated. eGFP and hSEAP production peaked at 72 hpt, with the majority of eGFP retained intracellularly whereas hSEAP (23.6 ± 2.3 mg/L) was mainly secreted to the supernatant (Fig. 4c). On the other hand, a continuous increase in Gag-eGFP production after transfection was measured by spectrofluorometry in the supernatant, with a significant amount of the polyprotein accumulated in the intracellular space and not budding in the form of VLPs. The sum of intracellular and extracellular Gag-eGFP production reached a maximum between 48 – 72 hpt. Confocal microscopy analysis of eGFP and Gag-eGFP transfected Sf9 cells showed the distinctive features of each recombinant product (Fig. 4d – e). In fact, all the green signal was localized intracellularly in eGFP producing cells. Conversely, yellow regions were observed in the membrane of Gag-eGFP transfected cells resulting from Gag-eGFP (green) and cell membrane (red) co-localization, a characteristic indication of VLP formation.

A more thorough characterization was conducted to assess the Gag-eGFP VLP production process. Flow virometry revealed that the maximal VLP concentration was attained at 48 hpt which differed from the data analyzed by spectrofluorometry (Fig. 4f). Non-assembled Gag-eGFP release could explain the increase of fluorescence in the supernatant but not in the form of

assembled nanoparticles. An increase in extracellular vesicle (EV) production was also detected by flow virometry and NTA (Table 3), which are known to be produced as a mechanism of cell-to-cell communication in different cell lines (Meckes and Raab-Traub, 2011). According to these results, 48 hpt proved to be the best option for VLP harvesting since the highest yield of VLPs and ratio of VLP to extracellular vesicles was obtained. In these conditions, a maximum VLP concentration of $1.9 \pm 0.8 \times 10^9$ VLP/mL was quantified by NTA.

3.5 Characterization of VLP production

A final characterization was performed to determine the efficiency of Sf9 cells at assembling Gag-eGFP in the form of VLPs (VLP fluorescence/ total fluorescence). To evaluate this, Gag-eGFP supernatants were ultracentrifuged in a double 25 – 45 % sucrose cushion and each of the resulting fractions was analyzed by spectrofluorometry (Fig. 5). The 80 % of the fluorescence signal measured was in the form of VLPs (25 %, 25 – 45 %, 45 % fractions) whereas the remaining 20 % corresponded to unassembled Gag-eGFP monomer (SN, SN – 25 %) or was associated to remaining cell debris (Pellet). Interestingly, the correlation of Gag-eGFP VLPs based on fluorescence (Eq. 2) resulted in $1.5 \pm 0.2 \times 10^9$ VLP/mL, which was in agreement with the VLP yield measured by NTA. These data indicated that VLP concentration could be accurately calculated using spectrofluorometry, which has been demonstrated to be a rapid and cost-effective quantification method (Gutiérrez-Granados et al., 2013).

4. Discussion

The insect cell/BEVS has proven to be a powerful tool for the expression of various recombinant proteins and complex nanoparticles. However, there are several limitations to this system associated to the lytic nature of infection that can influence product quality (Liu et al., 2013). Actually, production of complex nanoparticles such as VLPs can be compromised to some extent by the presence of baculovirus-derived proteins like GP64 (Luo et al., 2013). Although some efforts have been devoted to remove the co-expression of these proteins (Chaves

et al., 2018), the baculovirus itself still hampers VLP separation at the downstream stage (Vicente et al., 2011). Therefore, the use of alternative methodologies is of general interest. Here, we described a robust TGE method for the Sf9 cell line in a low-hydrolysate medium based on the transfection reagent polyethylenimine.

Initial efforts to transfect Sf9 cells were performed at low cell densities but resulted in poor transfection efficiencies and in cell cytotoxicity owing to increasing PEI concentrations. This cell line proved to be resistant to PEI transfection using standard approaches otherwise successfully applied in mammalian (Derouazi et al., 2004) and High Five cells (Mori et al., 2017). Better transfection yields maintaining high cell viabilities were obtained after medium replacement prior to transfection and using high cell density cultures. By doing so, the ratio of PEI/cell could be maintained at a low level while increasing the effective PEI concentration. Medium replacement has worked in several cases arguing that negatively-charged by-products are removed, thus avoiding their interference with DNA:PEI polyplexes (Rajendra et al., 2012; Ye et al., 2009). Moreover, some benefit has been reported with transfection at high cell densities since it is possible to increase the effective PEI concentration while maintaining a non-toxic PEI/cell ratio (Backliwal et al., 2008). Although it is relatively easy to perform medium replacement by centrifugation of small volumes, the same methodology could not be feasible at bioreactor scale. Alternatively, the adoption of perfusion strategies such as the alternating tangential flow (ATF) system are more convenient, as recently demonstrated in the development of a TGE-based bioprocess for influenza vaccine production in HEK 293 cells (Hong et al., 2019).

Medium replacement did not result in an additional stress to Sf9 cells, but the decrease in cell viability during the first 24 hpt was due to the transfection efficiency achieved and thus depending on the incubation solution selected for DNA and PEI complexing (Figure 1a, no transfection). The Sf900III medium and the 150 mM NaCl solution were not efficient in delivering the polyplexes to cells probably due to the fast aggregation kinetics between DNA and PEI in salt-containing solutions (Sang et al., 2013). In fact, big polyplexes can hinder the

uptake of DNA as recently demonstrated for High Five cells, where smaller DNA:PEI polyplexes were more efficient in achieving the highest transfection yields (Puente-Massaguer et al., 2018). Ultrapure water proved to be the best incubation solution to generate the DNA:PEI polyplexes. These polyplexes were stable in time with no differences regarding their transfection efficiency, which is in accordance with results reported by Shen and co-workers (Shen et al., 2013). However, these data differ from our previous study with High Five cells where the 150 mM NaCl incubation solution was selected for DNA and PEI complexing (Puente-Massaguer et al., 2018). Such differences are probably associated to the higher DNA and PEI effective concentrations required for an efficient transfection of Sf9 cells, hindering the use of this complexing solution since the aggregation kinetics would be too fast (Puente-Massaguer et al., 2018). Moreover, DNA:PEI polyplex size measured by cryo-TEM in the optimal conditions proved to be different, with polyplexes being more size heterogeneous for Sf9 cells. Additional studies should be conducted to determine whether a subpopulation of these polyplexes mediate a better transfection of Sf9 cells, or if this cell line can incorporate polyplexes with different sizes.

Several key parameters were monitored during TGE optimization using DoE. Cell viability after transfection, eGFP production and transfection were considered as crucial for proper process development. A multiple response optimization approach was applied to find a global TGE condition based on the three equations from the Box-Behnken DoE. Using this strategy, an optimal DNA/PEI ratio of 1:2 was found for Sf9 cells, similarly to transfection conditions reported for CHO (Bertschinger et al., 2008) and HEK 293 cells (Cervera et al., 2013).

The maximum eGFP yield achieved was 11.7 ± 0.5 mg/L at 3 days post transfection, a 2 and 2.7-fold increase compared to High Five and HEK 293SF cells (Puente-Massaguer et al., 2018), respectively, and 2-fold in terms of specific productivity (0.6 µg/10^6 transfected cells·day) with respect to lipofectin-based Sf9 cell transfection (Bleckmann et al., 2016b). Different results were observed when comparing this system to the Sf9/BEVS, with more than a 10-fold increase (Monteiro et al., 2014) or 6-fold decrease (Fernandes et al., 2012) in eGFP specific

productivities. Regarding hSEAP, Sf9 cells proved to be more efficient in producing this protein compared to eGFP, with a specific productivity of 1.1 ± 0.1 µg/10^6 transfected cells·day. The maximum hSEAP yield attained (23.6 ± 2.3 mg/L) was in the range of the 39 mg/L obtained with the Sf9/BEVS (Ikonomou et al., 2001).

From the perspective of new generation vaccines, we tested the utility of this platform to produce HIV-1 VLPs. The complexity associated to the production of Gag-eGFP could be clearly observed when comparing the fluorescence yields obtained with eGFP. Actually, a 15-fold increase in eGFP production (723.4 ± 40.5 R.F.U.) was achieved compared to Gag-eGFP (47.9 ± 12.1 R.F.U.). The budding process step required for VLP formation was found to be the bottleneck as demonstrated by spectrofluorometry and ELISA quantification of the intra- and extracellular Gag-eGFP levels (Table 3). Similar results have been observed in the production of Gag-eGFP VLPs in mammalian cells (González-Domínguez et al., 2020a), which highlights the difficulties of animal cells to process these complex nanoparticles. Still, the evaluation of the VLP assembly capacity of Sf9 cells by analytical ultracentrifugation revealed that this cell line was highly efficient since most of the polyprotein in the supernatant was in the form of assembled nanoparticles. These results are in the range of the 74 % Gag-eGFP VLP assembly efficiency reported in transfected HEK 293 cells at 48 hpt (Gutiérrez-Granados et al., 2013). In this sense, Sf9 cells provide an efficient platform for the production of VLPs with lower culture requirements and a higher level of safety. Analysis of VLP production by NTA and flow virometry revealed that extracellular vesicles (EVs) were co-produced with VLPs. Nanoparticles were even measured at the initial phase of transfection, possibly indicating that hydrolysates from Sf900III medium contribute to increase the levels of total nanoparticles detected (Puente-Massaguer et al., 2020c). The impact of EVs on biotechnological processes is still not fully understood and most of the work conducted so far has been performed in mammalian cells (Lee et al., 2019). Therefore, further efforts are required to comprehend their influence on insect cell-based processes.

The optimal transfection method developed in this work allowed to achieve a maximum VLP production of 1.9 ± 0.8 x 10^9 Gag-eGFP VLP/mL, representing a 2.8-fold increase compared to the initial condition. Interestingly, VLP quantification by flow virometry resulted in lower yields compared to NTA, which could be related to a different sensitivity level between techniques (González-Domínguez et al., 2020b).In addition, studies conducted by van der Pol *et al.* mention that it is possible that flow virometry detects sets of small nanoparticles as single larger nanoparticles, which could decrease the total number of particles quantified (Van Der Pol et al., 2012). Overall, Gag-eGFP VLP production levels proved to be in the range of HEK 293 cells by TGE (Cervera et al., 2013) and allowed a faster and also higher production by 3.9-fold in comparison to stable Sf9 cell lines (Vidigal et al., 2018). Moreover, strategies based on targeted supplementation by production enhancers (Cervera et al., 2015) or modulating culture conditions (Fernandes et al., 2020) could also be applied to further increase VLP yields, which opens a window of possibilities for TGE in Sf9 cells Hence, these results represent an advance to existing insect cell-based production platforms devoid of baculovirus, with a potential applicability to produce an ample variety of recombinant products.

5. Acknowledgments

The authors would like to thank Dr. Paula Alves (Instituto de Biologia Experimental e Tecnológica, Oeiras, Portugal) and Dr. Julià Blanco (IrsiCaixa, Badalona, Spain) for providing the pITV5 and pGag-eGFP plasmids, respectively. We would also like to thank Jorge Fomaro and Ángel Calvache (Beckman Coulter) for facilitating the access to the CytoFlex LX flow cytometer. The help of Núria Barba in confocal microscopy and Martí de Cabo with the cryo-TEM (Servei de Microscòpia, UAB) are also acknowledged. The support of José Amable Bernabé (Institut de Ciència de Materials de Barcelona, CSIC), Manuela Costa (Servei de Cultius Cel·lulars, Producció d'Anticossos i Citometria, UAB), Sahar Masoumeh Ghorbanpour (University of Natural Resources and Life Sciences, Vienna, Austria) and Llorenç Badiella (Servei d'Estadística Aplicada, UAB) with NTA, flow cytometry, ELISA quantification and

DoE, respectively, is appreciated. Eduard Puente-Massaguer is a recipient of an FPU grant from Ministerio de Educación, Cultura y Deporte of Spain (FPU15/03577). The research group is recognized as 2017 SGR 898 by Generalitat de Catalunya.

6. Compliance with Ethical Standards

6.1 Conflict of interest

The authors declare that they have no competing interests.

6.2 Ethical approval

This article does not contain any studies with human participants performed by any of the authors.

7. References

Backliwal, G., Hildinger, M., Hasija, V., Wurm, F.M., 2008. High-density transfection with HEK-293 cells allows doubling of transient titers and removes need for a priori DNA complex formation with PEI. Biotechnol. Bioeng. 99, 721–727.

Bertschinger, M., Schertenleib, A., Cevey, J., Hacker, D.L., Wurm, F.M., 2008. The kinetics of polyethylenimine-mediated transfection in suspension cultures of Chinese hamster ovary cells. Mol. Biotechnol. 40, 136–143.

Bleckmann, M., Schmelz, S., Schinkowski, C., Scrima, A., van den Heuvel, J., 2016a. Fast plasmid based protein expression analysis in insect cells using an automated SplitGFP screen. Biotechnol. Bioeng. 113, 1975–1983.

Bleckmann, M., Schürig, M., Chen, F.F., Yen, Z.Z., Lindemann, N., Meyer, S., Spehr, J., Van Den Heuvel, J., 2016b. Identification of essential genetic baculoviral elements for recombinant protein expression by transactivation in Sf21 insect cells. PLoS One 11, 1–19.

Bleckmann, M., Schürig, M., Endres, M., Samuels, A., Gebauer, D., Konisch, N., van den Heuvel, J., 2019. Identifying parameters to improve the reproducibility of transient gene expression in High Five cells. PLoS One 14, 1–18.

570 Carpentier, E., Lebesgue, D., Kamen, A.A., Hogue, M., Bouvier, M., Durocher, Y., 2001.
571 Increased production of active human β2-adrenergic/Gαs fusion receptor in Sf-9 cells
572 using nutrient limiting conditions. Protein Expr. Purif. 23, 66–74.
573 Cervera, L., Fuenmayor, J., González-Domínguez, I., Gutiérrez-Granados, S., Segura, M.M.,
574 Gòdia, F., 2015. Selection and optimization of transfection enhancer additives for
575 increased virus-like particle production in HEK293 suspension cell cultures. Appl.
576 Microbiol. Biotechnol. 99, 9935–9949.
577 Cervera, L., Gutiérrez-Granados, S., Martínez, M., Blanco, J., Gòdia, F., Segura, M.M., 2013.
578 Generation of HIV-1 Gag VLPs by transient transfection of HEK 293 suspension cell
579 cultures using an optimized animal-derived component free medium. J. Biotechnol. 166,
580 152–165.
581 Chaves, L.C.S., Ribeiro, B.M., Blissard, G.W., 2018. Production of GP64-free virus-like
582 particles from baculovirus-infected insect cells. J. Gen. Virol. 99, 265–274.
583 Derouazi, M., Girard, P., Van Tilborgh, F., Iglesias, K., Muller, N., Bertschinger, M., Wurm,
584 F.M., 2004. Serum-free large-scale transient transfection of CHO cells. Biotechnol.
585 Bioeng. 87, 537–545.
586 Fernandes, B., Vidigal, J., Correia, R., Carrondo, M.J.T., Alves, P.M., Teixeira, A.P., Roldão,
587 A., 2020. Adaptive laboratory evolution of stable insect cell lines for improved HIV-Gag
588 VLPs production. J. Biotechnol. 307, 139–147.
589 Fernandes, F., Vidigal, J., Dias, M.M., Prather, K.L.J., Coroadinha, A.S., Teixeira, A.P., Alves,
590 P.M., 2012. Flipase-mediated cassette exchange in Sf9 insect cells for stable gene
591 expression. Biotechnol. Bioeng. 109, 2836–2844.
592 Geisse, S., 2009. Reflections on more than 10 years of TGE approaches. Protein Expr. Purif. 64,
593 99–107.
594 George, S., Jauhar, A.M., Mackenzie, J., Kielich, S., Aucoin, M.G., 2015. Temporal
595 characterization of protein production levels from baculovirus vectors coding for GFP and
596 RFP genes under non-conventional promoter control. Biotechnol. Bioeng. 112, 1822–

1831.

González-Domínguez, I., Puente-Massaguer, E., Cervera, L., Gòdia, F., 2020a. Quantification of the HIV-1 virus-like particle production process by super-resolution imaging: From VLP budding to nanoparticle analysis. Biotechnol. Bioeng.

González-Domínguez, I., Puente-Massaguer, E., Cervera, L., Gòdia, F., 2020b. Quality Assessment of Virus-Like Particles at Single Particle Level: A Comparative Study. Viruses 12, 223.

Gutiérrez-Granados, S., Cervera, L., Gòdia, F., Carrillo, J., Segura, M.M., 2013. Development and validation of a quantitation assay for fluorescently tagged HIV-1 virus-like particles. J. Virol. Methods 193, 85–95.

Gutiérrez-Granados, S., Cervera, L., Kamen, A.A., Gòdia, F., 2018. Advancements in mammalian cell transient gene expression (TGE) technology for accelerated production of biologics. Crit. Rev. Biotechnol. 38, 918–940.

Gutierrez, J.M., Lewis, N.E., 2015. Optimizing eukaryotic cell hosts for protein production through systems biotechnology and genome-scale modeling. Biotechnol. J. 10, 939–949.

Hacker, D.L., Kiseljak, D., Rajendra, Y., Thurnheer, S., Baldi, L., Wurm, F.M., 2013. Polyethyleneimine-based transient gene expression processes for suspension-adapted HEK-293E and CHO-DG44 cells. Protein Expr. Purif. 92, 67–76.

Hong, J., Demirji, J., Blackstock, D., Lee, J., Dinh, T., Goh, A., Arnold, F., Horwitz, J., 2019. Development of an alternating tangential flow (ATF) perfusion-based transient gene expression (TGE) bioprocess for universal influenza vaccine. Biotechnol. Prog. 35, 1–9.

Ikonomou, L., Bastin, G., Schneider, Y.J., Agathos, S.N., 2001. Design of an efficient medium for insect cell growth and recombinant protein production. Vitr. Cell. Dev. Biol. - Anim. 37, 549–559.

Ikonomou, L., Schneider, Y.J., Agathos, S.N., 2003. Insect cell culture for industrial production of recombinant proteins. Appl. Microbiol. Biotechnol. 62, 1–20.

Keith, M.B., Farrell, P.J., Iatrou, K., Behie, L.A., 1999. Screening of transformed insect cell

lines for recombinant protein production. Biotechnol. Prog. 15, 1046–1052.

Lee, S.S., Won, J.H., Lim, G.J., Han, J., Lee, J.Y., Cho, K.O., Bae, Y.K., 2019. A novel population of extracellular vesicles smaller than exosomes promotes cell proliferation. Cell Commun. Signal. 17, 1–15.

Lin, S.Y., Chung, Y.C., Hu, Y.C., 2014. Update on baculovirus as an expression and/or delivery vehicle for vaccine antigens. Expert Rev. Vaccines 13, 1501–1521.

Liu, C., Dalby, B., Chen, W., Kilzer, J.M., Chiou, H.C., 2008. Transient transfection factors for high-level recombinant protein production in suspension cultured mammalian cells. Mol. Biotechnol. 39, 141–153.

Liu, F., Wu, X., Li, L., Liu, Z., Wang, Z., 2013. Use of baculovirus expression system for generation of virus-like particles: Successes and challenges. Protein Expr. Purif. 90, 104–116.

Lu, M., Johnson, R.R., Iatrou, K., 1996. Trans-activation of a cell housekeeping gene promoter by the IE1 gene product of baculoviruses. Virology 218, 103–113.

Luo, W.-Y., Lin, S.-Y., Lo, K.-W., Lu, C.-H., Hung, C.-L., Chen, C.-Y., Chang, C.-C., Hu, Y.-C., 2013. Adaptive Immune Responses Elicited by Baculovirus and Impacts on Subsequent Transgene Expression In Vivo. J. Virol. 87, 4965–4973.

Meckes, D.G., Raab-Traub, N., 2011. Microvesicles and Viral Infection. J. Virol. 85, 12844–12854.

Monteiro, F., Bernal, V., Saelens, X., Lozano, A.B., Bernal, C., Sevilla, A., Carrondo, M.J.T., Alves, P.M., 2014. Metabolic profiling of insect cell lines: Unveiling cell line determinants behind system's productivity. Biotechnol. Bioeng. 111, 816–828.

Mori, K., Hamada, H., Ogawa, T., Ohmuro-Matsuyama, Y., Katsuda, T., Yamaji, H., 2017. Efficient production of antibody Fab fragment by transient gene expression in insect cells. J. Biosci. Bioeng. 124, 221–226.

Nika, L., Wallner, J., Palmberger, D., Koczka, K., Vorauer-Uhl, K., Grabherr, R., 2017. Expression of full-length HER2 protein in Sf9 insect cells and its presentation on the

surface of budded virus-like particles. Protein Expr. Purif. 136, 27–38.

Puente-Massaguer, E., Lecina, M., Gòdia, F., 2020a. Application of advanced quantification techniques in nanoparticle-based vaccine development with the Sf9 cell baculovirus expression system. Vaccine 38, 1849–1859.

Puente-Massaguer, E., Lecina, M., Gòdia, F., 2020b. Integrating nanoparticle quantification and statistical design of experiments for efficient HIV-1 virus-like particle production in High Five cells. Appl. Microbiol. Biotechnol. 104, 1569–1582.

Puente-Massaguer, E., Lecina, M., Gòdia, F., 2018. Nanoscale characterization coupled to multi-parametric optimization of Hi5 cell transient gene expression. Appl. Microbiol. Biotechnol. 102, 10495–10510.

Puente-Massaguer, E., Saccardo, P., Ferrer-Miralles, N., Lecina, M., Gòdia, F., 2020c. Coupling microscopy and flow cytometry techniques for a comprehensive characterization of nanoparticle production in insect cells. Cytom. Part A.

Rajendra, Y., Kiseljak, D., Manoli, S., Baldi, L., Hacker, D.L., Wurm, F.M., 2012. Role of non-specific DNA in reducing coding DNA requirement for transient gene expression with CHO and HEK-293E cells. Biotechnol. Bioeng. 109, 2271–2278.

Reiter, K., Aguilar, P.P., Wetter, V., Steppert, P., Tover, A., Jungbauer, A., 2019. Separation of virus-like particles and extracellular vesicles by flow-through and heparin affinity chromatography. J. Chromatogr. A 1588, 77–84.

Sang, Y., Xie, K., Mu, Y., Lei, Y., Zhang, B., Xiong, S., Chen, Y., Qi, N., 2013. Salt ions and related parameters affect PEI–DNA particle size and transfection efficiency in Chinese hamster ovary cells. Cytotechnology 67, 67–74.

Schüpbach, J., Tomasik, Z., Knuchel, M., Opravil, M., Günthard, H.F., Nadal, D., Böni, J., 2006. Optimized virus disruption improves detection of HIV-1 p24 in particles and uncovers a p24 reactivity in patients with undetectable HIV-1 RNA under long-term HAART. J. Med. Virol. 78, 1003–1010.

Shen, X., Hacker, D.L., Baldi, L., Wurm, F.M., 2013. Virus-free transient protein production in

Sf9 cells. J. Biotechnol. 171, 61–70.

Shen, X., Pitol, A.K., Bachmann, V., Hacker, D.L., Baldi, L., Wurm, F.M., 2015. A simple plasmid-based transient gene expression method using High Five cells. J. Biotechnol. 216, 67–75.

Thompson, B.C., Segarra, C.R.J., Mozley, O.L., Daramola, O., Field, R., Levison, P.R., James, D.C., 2012. Cell line specific control of polyethylenimine-mediated transient transfection optimized with "Design of experiments" methodology. Biotechnol. Prog. 28, 179–187.

Van Der Pol, E., Van Gemert, M.J.C., Sturk, A., Nieuwland, R., Van Leeuwen, T.G., 2012. Single vs. swarm detection of microparticles and exosomes by flow cytometry. J. Thromb. Haemost. 10, 919–930.

Van Gaal, E.V.B., Van Eijk, R., Oosting, R.S., Kok, R.J., Hennink, W.E., Crommelin, D.J.A., Mastrobattista, E., 2011. How to screen non-viral gene delivery systems in vitro? J. Control. Release 154, 218–232.

Vicente, T., Roldão, A., Peixoto, C., Carrondo, M.J.T., Alves, P.M., 2011. Large-scale production and purification of VLP-based vaccines. J. Invertebr. Pathol. 107, S42–S48.

Vidigal, J., Fernandes, B., Dias, M.M., Patrone, M., Roldão, A., Carrondo, M.J.T., Alves, P.M., Teixeira, A.P., 2018. RMCE-based insect cell platform to produce membrane proteins captured on HIV-1 Gag virus-like particles. Appl. Microbiol. Biotechnol. 102, 655–666.

Ye, J., Kober, V., Tellers, M., Naji, Z., Salmon, P., Markusen, J.F., 2009. High-level protein expression in scalable CHO transient transfection. Biotechnol. Bioeng. 103, 542–551.

8. Figure captions

Figure 1. Transfection and eGFP production process in Sf9 cells in batch culture with DNA:PEI polyplexes pre-formed in ultrapure water, 150 mM NaCl, Sf900III medium and direct addition of PEI + DNA (no complexing). (a) Cell growth and viability profile of transfected cultures. Exponentially growing cells were transfected at 20 x 10^6 cells/mL and diluted to 4 x 10^6 cells/mL after 1 h. (b – c) Transfection yield and median fluorescence intensity of transfected cells analyzed by flow cytometry. (d) Intracellular eGFP production measured with spectrofluorometry. Mean values ± standard deviation of triplicate experiments are represented.

Figure 2. DNA:PEI polyplex characterization and their effect in high cell density cultures. (a – b) Cryo-transmission electron microscopy images of DNA:PEI polyplexes pre-formed in ultrapure water for < 1 min. (c – d) Cell growth and TGE levels of DNA:PEI polyplexes maintained during different incubation times with high cell density cultures. Mean values ± standard deviation of triplicate experiments are represented.

Figure 3. Response surface graphs from Box-Behnken DoE. (a – c) Intracellular eGFP production as a function of viable cell concentration, DNA/cell and PEI/cell ratios at 72 hpt. (d – f) Percentage of eGFP positive cells as a function of viable cell concentration, DNA/cell and PEI/cell ratios at 72 hpt. (g – i) Cell culture viability as a function of viable cell concentration, DNA/cell and PEI/cell ratios at 24 hpt. Three-dimensional graphs were constructed by depicting two variables at a time and maintaining the third one at a fixed level.

Figure 4. Validation of the global optimal conditions and comparison to hSEAP and Gag-eGFP VLP production. (a) Cell growth and viability profile of transfected cultures producing different recombinant products. Exponentially growing cells were transfected at 17.6 x 10^6 cells/mL and diluted to 4 x 10^6 cells/mL after 15 min. (b – c) Transfection yield and intracellular/extracellular production of the different recombinant products. (d – e) Fluorescence confocal microscopy image of pIZTV5-eGFP (d) and pIZTV5-Gag-eGFP (e) transfected Sf9 cells. Cell nucleus was stained with Hoechst 33342 (blue) and membrane was stained with CellMask™ (red). (f) Nanoparticle quantification of Gag-eGFP VLP producing cells by flow virometry. The average values of triplicate experiments are represented.

Figure 5. Gag-eGFP supernatant characterization by spectrofluorometry. Fluorescence distribution of Gag-eGFP supernatant harvested at 48 hpt after double sucrose cushion ultracentrifugation. Mean values ± standard deviation of triplicate experiments are represented.

FIGURES

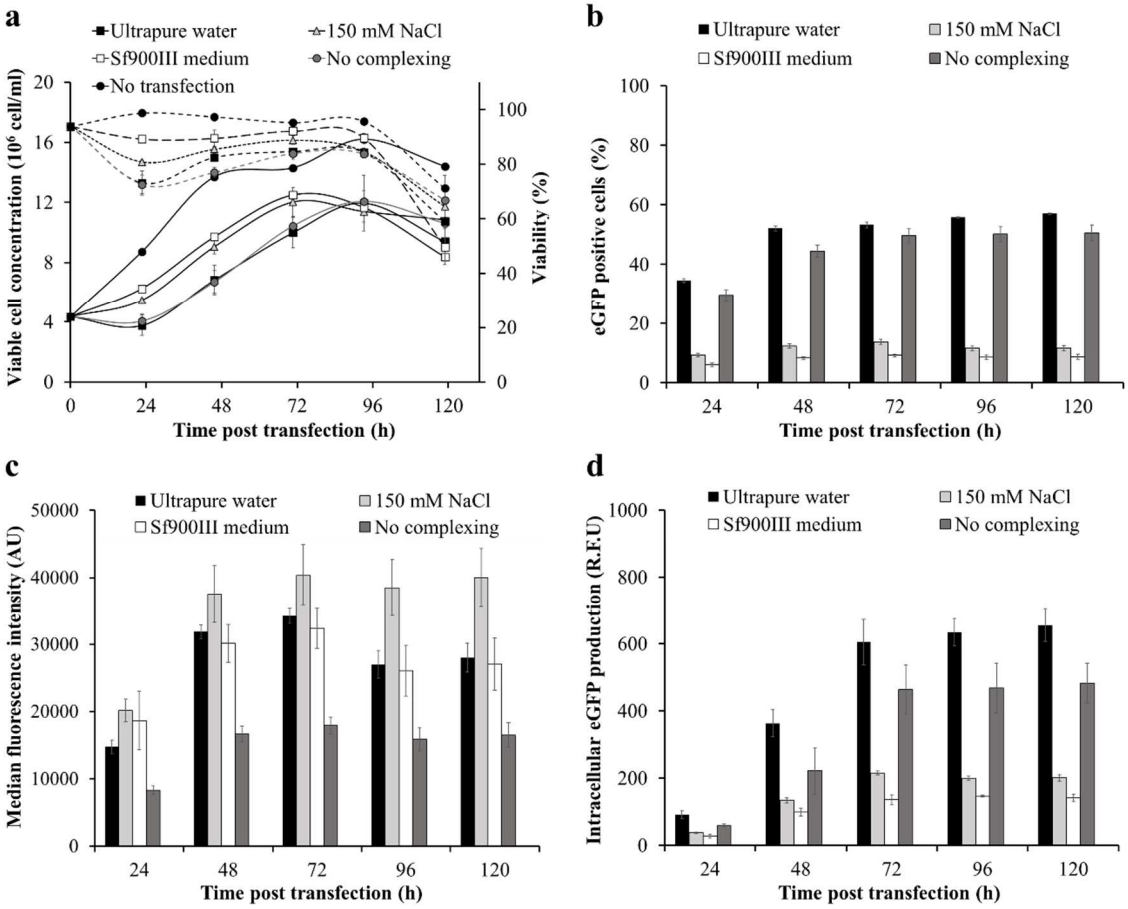

Figure 1

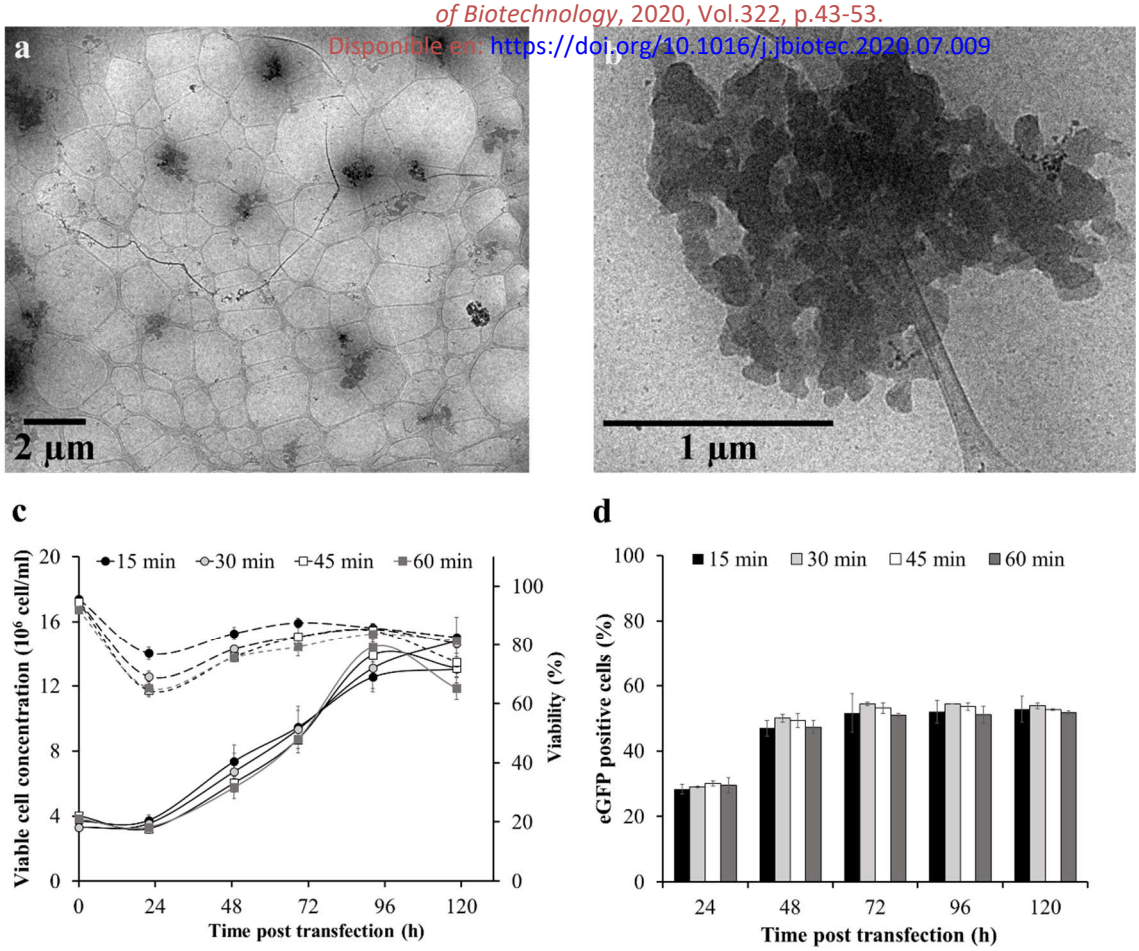

Figure 2

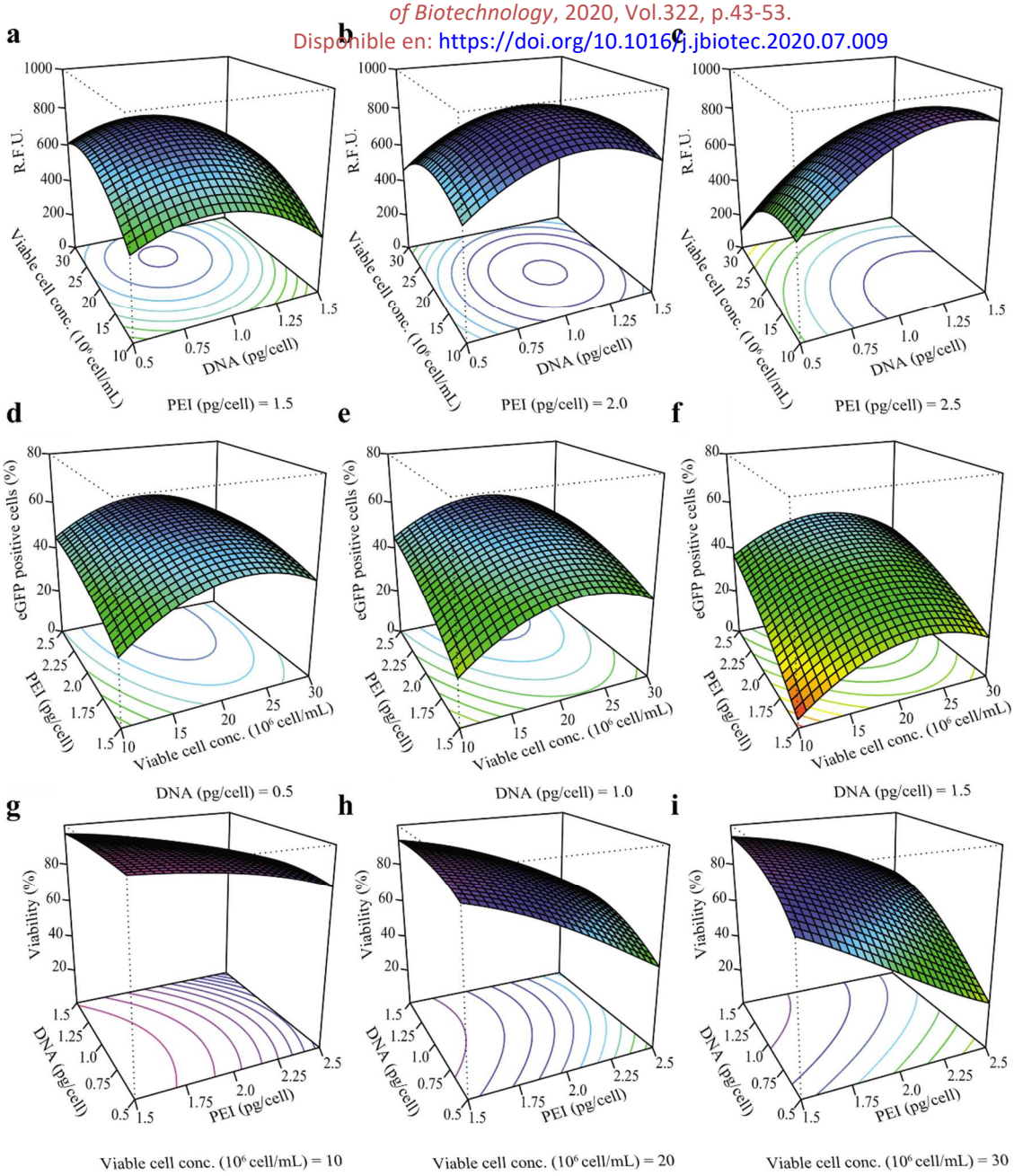

Figure 3

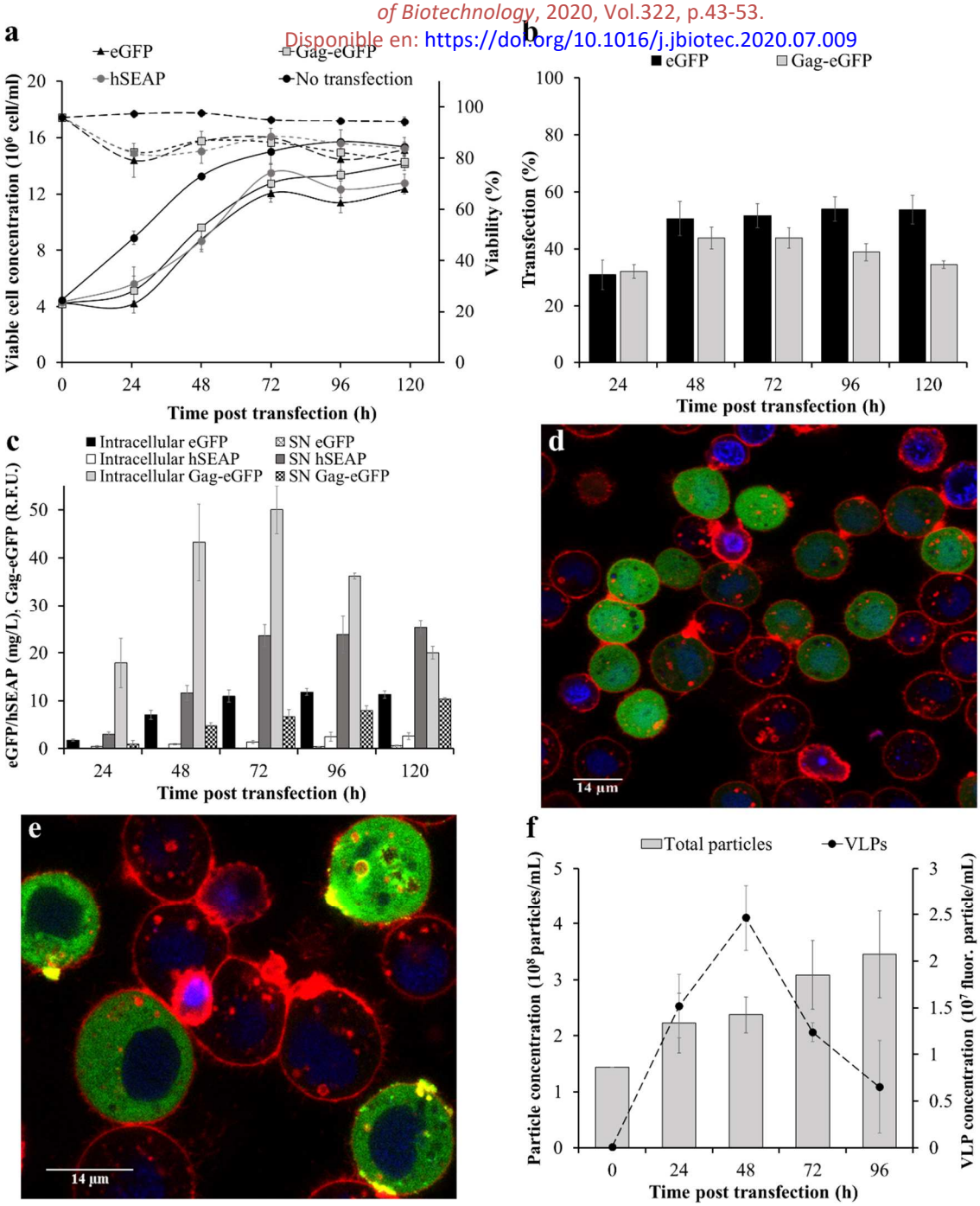

Figure 4

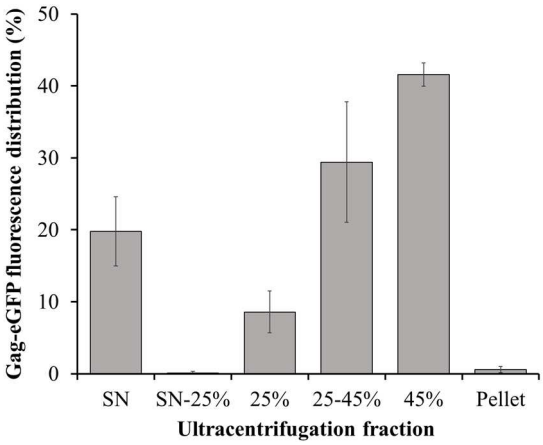

Figure 5

TABLES AND CORRESPONDING TITLES

Table 1. Matrix design, response and ANOVA analysis for the Box-Behnken DoE variables. Run 13 was performed in triplicate as the centre point.

Coded levels	-1	0	1
Viable cell concentration (10^6 cell/mL)	10	20	30
DNA:cell ratio (pg/cell)	0.5	1	1.5
PEI:cell ratio(pg/cell)	1.5	2	2.5

	Variables			Responses		
Experimental run	[Cell][a]	DNA:cell ratio	PEI:cell ratio	Specific production (R.F.U./10^6 cells)	eGFP positive cells (%)	Viability (%)
1	-1	-1	0	109.5	38.0	93.8
2	1	-1	0	89.1	47.9	55.8
3	-1	1	0	197.3	22.7	85.6
4	1	1	0	150.3	33.0	83.1
5	-1	0	-1	147.9	20.7	96.7
6	1	0	-1	133.6	31.6	90.7
7	-1	0	1	146.6	45.5	88.4
8	1	0	1	118.0	45.0	48.7
9	0	-1	-1	119.8	46.5	87.1
10	0	1	-1	177.5	22.3	93.7
11	0	-1	1	99.1	59.1	30.1
12	0	1	1	124.5	50.2	62.5
13	0	0	0	130.6	55.0	84.8
13	0	0	0	140.1	50.1	82.4
13	0	0	0	120.6	52.0	78.9

Model	*F* test, *p*-value	Lack of fit test, *p-value*[b]	R^2	Adjusted R^2
eGFP production (72 hpt)	0.048	0.053	84.9	64.8
eGFP positive cells (72 hpt)	<0.001	0.72	98.8	97.2
Viability (24 hpt)	<0.001	0.28	94.4	90.2

Model	eGFP production (72hpt)		eGFP positive cells (72 hpt)		Viability (24hpt)	
Parameters	Coefficient	*p*-value	Coefficient	*p*-value	Coefficient	*p*-value
Constant	848.550	<0.001	52.2367	<0.001	1.487	<0.001
[Cell]	-44.790	0.264	3.825	0.002	-0.732	<0.001
$[Cell]^2$	-122.000	0.063	-12.896	<0.001	0.4516	0.041
[DNA]	63.510	0.131	-7.913	<0.001	0.321	0.034
$[DNA]^2$	-160.710	0.024	-4.071	0.009	-0.388	0.070
[PEI]	14.930	0.695	9.838	<0.001	-1.077	<0.001
$[PEI]^2$	-100.460	0.109	-3.771	0.01	NS	>0.050
[Cell] x [DNA]	NS	>0.050	NS	>0.050	0.574	0.010
[Cell] x [PEI]	-140.220	0.034	-2.850	0.03	NS	>0.050
[DNA] x [PEI]	125.720	0.05	3.825	0.01	NS	>0.050

[a][Cell]: viable cell concentration

[b]Lack of fit test, *p*-value above 0.05 imply that the hypothesis arguing that the model is suitable cannot be rejected.

NS: non-significant term (*p-value* > 0.05)

Table 2. Experimental validation of the optimal TGE condition and comparison to model predictions.

Response	Experimental	Model prediction
eGFP positive cells (%)	51.7 ± 4.3	52.0 ± 2.1
eGFP production (mg/L)	11.7 ± 0.5	13.7 ± 1.8
Viability (%)	79.1 ± 6.7	83.0 ± 5.5

Table 3. GageGFP production in harvested supernatants and cell lysates at 48 hpt using different quantification methodologies.

Quantification method	Fluorescent particles/mL	Total particles/ mL	Supernatant	Intracellular
NTA (particles/mL)	$1.9 \pm 0.8 \cdot 10^{9}$	$7.5 \pm 0.1 \cdot 10^{10}$	-	-
Flow virometry (particles/mL)	$2.5 \pm 0.4 \cdot 10^{7}$	$2.4 \pm 0.3 \cdot 10^{8}$	-	-
ELISA (ng/mL)	-	-	41.9	211.1
Fluorometry (R.F.U.)	$1.5 \pm 0.2 \cdot 10^{9}$[a]	-	4.8 ± 0.6	43.1 ± 11.5

[a]This is the resulting value of correlating R.F.U. to NTA (eq. 2)